

# Adsorption kinetics of $\beta$ -lactoglobulin on a polyclonal immunochromatographic support

Angel Puerta<sup>a</sup>, Alain Jaulmes<sup>b</sup>, Mercedes De Frutos<sup>a</sup>, Jose Carlos Diez-Masa<sup>a</sup>, Claire Vidal-Madjar<sup>b</sup>

a) Instituto de Química Orgánica (C.S.I.C.), Juan de la Cierva 3, 28006 Madrid, Spain

b) Laboratoire de Recherche sur les Polymères, CNRS, 2 Rue Henry Dunant, 94320 Thiais, France

**Keywords:** Adsorption kinetics, Kinetic studies, Immunoabsorbents, Proteins, Lactoglobulins

**Correspondence:** M. de Frutos, Instituto de Química Orgánica (C.S.I.C.), Juan de la Cierva 3, 28006 Madrid, Spain. **E-mail:** mfrutos@iqog.csic.es

**Abstract**

$\beta$ -Lactoglobulin is one of the main components of whey proteins. Among other reasons, its allergenicity makes its determination in hypoallergenic foods and bio-pharmaceutical products necessary. Immunoaffinity chromatography is a widely accepted technique for purification and analysis of proteins. Knowledge of the apparent kinetics of the adsorption of  $\beta$ -lactoglobulin onto the anti- $\beta$ -lactoglobulin immunochromatographic column is important to optimize the analytical process. High-performance frontal affinity chromatography was used to study the apparent kinetics of the adsorption process. Langmuir and bi-Langmuir kinetic models, assuming one and two kinds of binding sites, respectively, were used to characterize the adsorption kinetics of  $\beta$ -lactoglobulin B on a polyclonal immunoadsorbent. Very good fits were obtained with the bi-Langmuir model for two different concentrations of  $\beta$ -lactoglobulin and this allowed us to calculate the apparent adsorption rate constants and the column capacities for both kinds of sites. Experimental results indicate the possibility that the adsorption process is not irreversible. The values of the apparent dissociation rate constants leading to the best fit were estimated and the affinity constants were calculated.

## 1. Introduction

$\beta$ -Lactoglobulin ( $\beta$ -LG) is one of the main proteins in the whey fraction of milk. Its determination in different nutritional and bio-pharmaceutical products has been carried out by several methods, most of them based on separation techniques. Analytical protocols using high-performance liquid chromatography (HPLC) and capillary electrophoresis (CE) allow fast separation and precise quantitation of this protein. However, these methods are not sensitive enough for the determination of  $\beta$ -LG at trace levels. The main interest of measuring such low levels of  $\beta$ -LG is its allergenic character. In fact,  $\beta$ -LG is considered as one of the main factors causing allergic reactions to bovine milk, especially in infants [1]. Hypoallergenic food products intended to be  $\beta$ -LG free have been commercialized as substitutes of milk for allergic people. Unfortunately, even minor residual amounts of  $\beta$ -LG have caused allergic reactions. Besides that, the production of bio-pharmaceutical products in the milk of transgenic cows developed in the last years demands the determination of  $\beta$ -LG at low levels in the quality control assays for the therapeutic protein due to the allergenic character of  $\beta$ -LG [2].

Due to the specificity of the antigen–antibody interactions, methods based on immunorecognition are very selective. Immunorecognition methods carried out in chromatographic columns can be used for both isolation and analysis of  $\beta$ -LG. In immunochromatographic columns, antibodies raised against  $\beta$ -LG are covalently bound to the chromatographic packing. Samples are passed through the column, where  $\beta$ -LG is captured and concentrated by the anti- $\beta$ -LG antibodies while the rest of components of the samples are eluted unretained. The retained  $\beta$ -LG can then be eluted and analyzed by other techniques (for example immunoassay) or it can be analyzed in-situ by, for example, performing an enzyme-linked immunosorbent assay (ELISA) inside the column. This kind of assay has proven to provide very high sensitivity [3] and this is of interest for determining trace amounts of compounds. In order to optimize immunochromatographic processes, knowledge of the kinetics of the adsorption process is useful [4], [5]. Frontal affinity chromatography, especially in the high-performance (HPLC) format has been demonstrated to be a good method for performing these studies [6], [7].

Several theoretical approaches have been developed to describe the chromatographic process in the frontal elution mode. These models were used to estimate the adsorption–desorption rate constants of proteins on immunoadsorbents by fitting the theoretical profiles to the experimental breakthrough curves [6]. Numerical simulation models account for the different rate-controlling mechanisms [8], [9]: the film mass-transfer resistance, the diffusion of the protein into the pores and the interaction with the adsorption sites. In practice, it is difficult to apply such an approach because the number of parameters is large, which does not allow one to discriminate between the various contributions. Moreover, these models generally assume an adsorption isotherm of the Langmuir type and thus a homogeneous distribution of binding sites. In the simplified analytical approaches, the adsorption process is described by a single binding rate equation of the Langmuir type [10], [11], implying apparent adsorption and desorption rate constants. Generally, such a model does not represent well the experimental profile, as large discrepancies between the theoretical and experimental breakthrough curves occur at larger solute concentrations when the front slowly reaches its asymptotic value.

Recently, we used a model based on bi-Langmuir type kinetics to analyze the adsorption kinetics of human serum albumin (HSA) on an anti-HSA monoclonal antibody immobilized on a silica support [12]. The model assumes a heterogeneous adsorbent with two types of binding sites and yields an equilibrium adsorption isotherm of the bi-Langmuir type. In the case of extremely low desorption rates, the model allows the determination of the saturation capacities of the sites of types 1 and 2 and the corresponding apparent adsorption rates. These apparent constants describe, in global terms, the different rate-controlling mechanisms. These kinetic parameters were obtained from the best fit of the theoretical front to the experimental breakthrough curves.

The aim of this work is to apply the bi-Langmuir type kinetic model to characterize the adsorption kinetics of  $\beta$ -LG on a polyclonal immunoadsorbent. It is known that the different genetic variants of bovine  $\beta$ -LG behave differently regarding conformational changes and aggregation [13]. As competitive effects may interfere in the adsorption mechanisms, we studied the retention behavior of a single protein instead of using a mixture of variants. The B variant was selected as its tendency to associate at pH 7.5 and 20 °C is lower than that of the A variant [14]. Unless otherwise stated,  $\beta$ -LG refers to bovine  $\beta$ -LG B.

On the other hand, the adsorbent surface is heterogeneous in terms of protein–protein interactivities, because a polyclonal antibody has been grafted on the chromatographic support. Moreover, interactions between  $\beta$ -LG and the solid support material cannot be excluded. A model considering only two types of binding sites gives an approximate picture of the sorbent heterogeneity, but it is certainly more appropriate than those based on simple Langmuirian kinetics. As the hypothesis of irreversible adsorption may not hold with many experimental systems, we will discuss the possibility of applying the bi-Langmuir type model to cases in which partial desorption occurs.

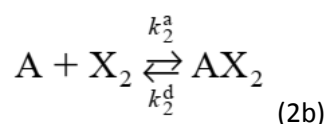
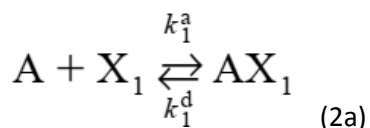
## 2. Theory

In this model, the column is divided into transversal slices of arbitrary thickness. The differential mass balance of a solute in a slice of column of volume  $\Delta v$  is given by [5]:

$$\frac{\partial c}{\partial t} + u \cdot \frac{\partial c}{\partial z} + \frac{1}{\epsilon \Delta v} \cdot \frac{\partial q}{\partial t} = D \cdot \frac{\partial^2 c}{\partial z^2} \quad (1)$$

where  $z$  is the abscissa along the column,  $u$  the mobile phase velocity,  $\epsilon$  the void volume fraction,  $c$  the solute concentration in the mobile phase and  $q$  the amount of solute in the particle. It includes the amount that is adsorbed and that is present in the pores. The axial dispersion coefficient in the mobile phase is  $D$ . It accounts for the contributions of molecular diffusion and eddy diffusion to band broadening. It is related [4] to the height equivalent to a theoretical plate (HETP) by  $D=H_D u/2$ .  $H_D$  is the contribution to band broadening in the absence of kinetic effects. The effect of molecular diffusion is negligible for proteins, because the value of the molecular diffusion coefficient in bulk liquid is around  $5 \cdot 10^{-6}$  cm<sup>2</sup>/s.

The mass-transfer exchanges of the solute on the non-uniform support involve two types of binding sites and are described by the following chemical equations:



where  $X_1$  and  $X_2$  represent the adsorption sites of types 1 and 2. The apparent adsorption rate constants are  $k_{a1}$  and  $k_{a2}$  and the apparent desorption rate constants are  $k_{d1}$  and  $k_{d2}$ . These apparent adsorption–desorption rate constants are empirical constants that describe, in global terms, both the adsorption–desorption process on the active sites and the other mass-transfer contributions, such as the film resistance around the particles and the diffusion into the pores of the support.

$q_1$  and  $q_2$  stand for the average amounts of solute adsorbed on the sites of types 1 and 2, with  $q = q_1 + q_2$ . If the corresponding saturation capacities are  $Q_1$  and  $Q_2$ , the system of chemical equations is ruled by the kinetic laws:

$$\frac{dq_1}{dt} = k_1^a c(Q_1 - q_1) - k_1^d q_1 \quad (3a)$$

$$\frac{dq_2}{dt} = k_2^a c(Q_2 - q_2) - k_2^d q_2 \quad (3b)$$

The equilibrium constants are given by  $K_1 = k_{a1}/k_{d1}$  and  $K_2 = k_{a2}/k_{d2}$ . If one considers the case where the exchanges are rapid enough to allow the use of equilibrium relations, the equilibrium isotherm can be expressed by setting  $dq_1/dt$  and  $dq_2/dt$  equal to zero. Considering the global adsorbed solute amount, the adsorption–desorption equilibrium isotherm is described in the final «bi-langmuirian» form:(4)

A numerical simulation procedure was used to generate the theoretical elution front by solving the system of differential equations describing the solute migration through the column and the adsorption process (Eqs. (1), (3a) and (3b)). The numerical procedure used is divided in two steps, the axial dispersion step according to Fick's law and the step for mass-transfer exchanges. The column is divided into a number of slices large enough to minimize numerical dispersion and thus render its contribution negligible compared to the experimental band broadening. Mass conservation is assumed in each step of the simulated chromatographic process. The numerical procedures for simulating Fick's law [5] and the mass transfer exchanges [12] have already been explained in previous papers.

### 3. Experimental

#### 3.1. Chemicals

Trizma base, Trizma hydrochloride, potassium chloride,  $\beta$ -lactoglobulin B (L-8005) ( $\beta$ -LG B) and  $\alpha$ -lactalbumin (L-6010) ( $\alpha$ -LA) were purchased from Sigma (St. Louis, MO, USA).

Magnesium chloride hexahydrate, sodium chloride, sodium dihydrogenphosphate, disodium hydrogenphosphate dihydrate, and potassium dihydrogenphosphate were from Merck (Darmstadt, Germany).

Sulfuric acid was purchased from Panreac (Barcelona, Spain). Sodium m-periodate was from Carlo Erba (Milan, Italy). Glycerol was obtained from Foret (Barcelona, Spain). Sodium azide was from J.T. Baker (Deventer, The Netherlands). Ethanolamine was purchased from Scharlau (Barcelona, Spain) and sodium cyanoborohydride from Aldrich (Milwaukee, WI, USA).

Affinity-purified anti-bovine  $\beta$ -LG (A+B) raised in rabbit was purchased from Bethyl Labs. (Montgomery, TX, USA).

All the buffers and solutions were prepared in Ultrapure water (resistivity 18.2 M $\Omega$  cm) obtained from a Milli-Q unit (Millipore, Bedford, MA, USA).

#### 3.2. Immunochromatographic column

Epoxy-silica (Waters Protein-Pak epoxy-activated affinity products) of 40  $\mu$ m particle size and 500 Å pore diameter was from Waters (Millipore, Waters Chromatography Division, Milford, MA, USA).

The derivatization of the epoxy-silica support, in order to immobilize the anti-bovine  $\beta$ -LG (A+B) on it, was performed through the transformation of the epoxy-silica into aldehyde-silica [15]. Briefly, epoxy-silica was converted to diol-silica by acid hydrolysis with diluted sulfuric acid. Diol-silica was oxidized to aldehyde-silica with sodium periodate and the oxidation reaction was stopped by the addition of glycerol.

Prior to coupling, the antibody was added to the coupling buffer (0.5 M phosphate, pH 6.9), and concentrated with centrifugal filter devices with Mr 50 000 cut-off membranes (Centricon 50,

Amicon, Beverly, MA, USA) by using a Biofuge 22R centrifuge (Heraeus Sepatech, Hanau, Germany). The antibody was immobilized on the support by suspending the aldehyde-silica in the coupling buffer containing it, in the presence of sodium cyanoborohydride in order to reduce the Schiff base after its formation during the coupling reaction. After 62 h at 4 °C and gentle mixing, the supernatant was decanted and 1 M ethanolamine solution at pH 9.5 in coupling buffer was added to block the unreacted aldehyde groups, being hold for 22 h. Finally, the blocking solution was removed and the antibody-silica was washed with coupling buffer and 1 M sodium chloride. A slurry of the antibody-silica beads in Tris-buffered saline (TBS=0.01 M Tris, 0.137 M NaCl, 0.0027 M KCl, pH 7.4) solution was packed into an empty stainless steel HPLC column (5 cm×2.1 mm) under high pressure using TBS as packing mobile phase. The efficiency of antibody coupling to the chromatographic support was indirectly calculated. The amount of antibody present in the solution before coupling and in the aliquots of the supernatant after the different coupling steps was calculated by measuring the absorbance at 280 nm.

### 3.3. Chromatographic device

The chromatographic system for frontal assays consisted of a LKB 2150 HPLC pump (LKB, Bromma, Sweden), a LKB 2152 HPLC controller, a LC-95 variable-wavelength UV–Vis detector (Perkin-Elmer, Norwalk, CT, USA) and a 7125 injection valve (Rheodyne, Cotati, CA, USA) equipped with a 5 ml sample loop. All the connecting tubes were made of stainless steel.

The signal from the detector was passed through an A/D converter Module 406 (Beckman Instruments, Fullerton, CA, USA) and data acquisition was performed with the System Gold program (version V810, Beckman Instruments) on an AMC 486 computer.

### 3.4. Chromatographic method

The mobile phase used was TBS. The regenerating eluent used for column recovery was a solution of 4 M magnesium chloride in 20 mM Tris buffer at pH 7.4.

Frontal analysis was performed by injecting onto the antibody column 5 ml of protein ( $\beta$ -LG B or  $\alpha$ -LA) solution in the mobile phase at a flow rate of 0.1 ml/min. The flow-rate was kept constant until the detector signal returned to baseline. Each frontal assay took 90 min to be performed.



Desorption with the regenerating eluent was carried out at 0.2 ml/min flow rate for 25 min, followed by 5 min at 0.5 ml/min.

The sequence of chromatographic processes was as follows: after cleaning the antibody column by injecting 3×1.2 ml of the regenerating solution at 0.2 ml/min, conditioning of the column was performed at 0.1 ml/min for 10 min. Then, 5 ml of a  $\beta$ -LG B solution was injected into the immunoabsorbent column. After 90 min, the frontal assay was completed and the initial baseline recovered. Subsequently, the flow-rate was kept at 0.1 ml/min for 30 min, as a rinsing step, in order to possibly elute  $\beta$ -LG B from the column. A second injection of  $\beta$ -LG B was then performed to test the ability of the column to retain  $\beta$ -LG B again. Two different concentrations of  $\beta$ -LG B, namely 0.00575 and 0.023 g/l were considered.

The immunochromatographic column was regenerated by the injection of 3×1.2 ml of the regenerating agent and an injection of 5 ml of  $\alpha$ -LA was carried out in order to determine the value of the column void volume ( $V_0=0.13$  ml). The  $\alpha$ -LA concentrations used were 0.00373 and 0.015 g/l in order to obtain absorbance values similar to those of diluted and concentrated  $\beta$ -LG B, respectively. At the end of each working day, the column was washed by injecting twice 1.2 ml of the regenerating solution, followed by 5 ml of a sodium azide solution 0.02% (w/v) in phosphate-buffered saline (0.01 M sodium phosphate, 0.138 M sodium chloride, 0.0027 M potassium chloride, pH 7.4) to prevent microorganism growth. The column was stored in the refrigerator (4 °C) overnight.

To better simulate the affinity interactions taking place in real immunochromatographic assays, the antibody-column was submitted to more than one hundred affinity assays before carrying out the frontal assays described in this work.

### **3.5. Fitting of theoretical and experimental profiles**

All simulation programs were written in Fortran language and run on a Dell Optiplex GX1L500 personal computer. A simplex method was used for best fitting, selecting the parameters which

generate a front for which the sum of the squares of the deviations ( $\Sigma$ ) between the theoretical and experimental profiles is minimum.

In the absence of kinetic effects, band broadening is mainly due to eddy diffusion. Considering an average particle diameter of 40  $\mu\text{m}$ , the eddy diffusion contribution to the HETP, calculated as indicated in Ref. [16], was  $H_D=0.030$  cm. From this value the axial dispersion coefficient ( $D=1\cdot 10^{-3}$   $\text{cm}^2/\text{s}$ ) for  $u=0.064$   $\text{cm}/\text{s}$  was estimated. When simulating the fronts with  $D=10^{-3}$   $\text{cm}^2/\text{s}$  this effect was hardly noticeable, much less important than the effect of the slow mass transfer kinetics observed. To lower the calculation time, we considered that the axial dispersion effect is negligible. The effect of numerical dispersion was minimized by dividing the column into a large number of slices (500), way above 50, the limit under which numerical dispersion effects start being noticed.

In the mass transfer adsorption–desorption simulation procedure, the apparent desorption rate constants ( $k_{d1}$  and  $k_{d2}$ ) were kept constant at various given values and the four parameters,  $k_{a1}$ ,  $k_{a2}$ ,  $Q_1$ , and  $Q_2$  were determined from the best fit obtained. In this work, the sites of type 1 were assigned to those of larger affinity constant.

#### 4. Results

Fig. 1 shows the experimental curves corresponding to the frontal loading of  $\beta$ -LG B and  $\alpha$ -LA. The emergence volume of  $\alpha$ -LA, a protein that should not be specifically retained by the immunochromatographic column is  $V_0$ , the column void volume. By comparison of the curves corresponding to the first frontal loading of  $\beta$ -LG and that of  $\alpha$ -LA it can be seen that  $\beta$ -LG is retained by the anti- $\beta$ -LG column. The differences in elution time at which each protein emerges indicate the extent of  $\beta$ -LG retention. If adsorption were irreversible, the saturated column would not be able to retain additional amounts of  $\beta$ -LG. In this case, a further injection of  $\beta$ -LG into the saturated column would lead to a profile identical to that of a non-retained protein ( $\alpha$ -LA). After rinsing the saturated column with the mobile phase for 30 min, a significant retention of  $\beta$ -LG is observed with the second frontal loading of a large amount of protein. One explanation could be a partial desorption of  $\beta$ -lactoglobulin-B from the column when the column is rinsed with the mobile phase buffer.

#### 4.1. Adsorption of a low concentration of $\beta$ -lactoglobulin B

Fig. 2 shows the breakthrough curve for a diluted solution of  $\beta$ -lactoglobulin B (0.00575 g/l) eluted from the immunoabsorbent column. A steep front is first observed, then a more diffuse part reaches slowly the asymptotic value, i.e., the protein feed concentration. The total amount of protein retained ( $q=4.3 \mu\text{g}$ ) was calculated from the area of the plot comprised between  $V_0$  and the breakthrough curve. After washing the column for 30 min with the mobile phase buffer, another frontal experiment is performed. A sharp front emerges from the column (Fig. 2) and the amount of protein adsorbed is  $q=3.5 \mu\text{g}$ , about 80% of the amount retained in the first adsorption step.

In a previous work [12], we assumed a negligible protein apparent desorption rate during the duration of a frontal experiment. For the adsorption of  $\beta$ -lactoglobulin on this immunoabsorbent, this hypothesis may not hold. As shown in Fig. 2, a second injection of  $\beta$ -lactoglobulin performed after rinsing the previously saturated column with mobile phase buffer led to the retention of protein. From the ratio of the amounts of protein adsorbed in first and second experiments, one can estimate a value for the desorption rate constant around  $10^{-3} \text{ s}^{-1}$  by assuming an exponential decay law for the quantity of protein retained. The values of  $k_1^d$  and  $k_2^d$  were fixed at  $10^{-3} \text{ s}^{-1}$  and the fitting of the theoretical profile to the experimental breakthrough curve was then performed to determine the other kinetic parameters: the capacities of the high and low affinity sites and the corresponding apparent adsorption rate constants (Table 1). Close values of column capacities between both kinds of sites are found for the bi-Langmuir model; the apparent adsorption rate on the sites of type 1 as well as the affinity constant is 10 times larger than on the type 2 sites. The values of the affinity constants  $K_1$  and  $K_2$  were calculated from the ratios of  $k_1^a/k_1^d$  and  $k_2^a/k_2^d$ .

If the surface interaction rate is described with a single chemical reaction (adsorption on a uniform adsorbent), the adsorption isotherm is of the Langmuir type. This model is described with three parameters ( $Q_1$ ,  $k_{a1}$ ,  $k_{d1}$ ) and the breakthrough curve is symmetrical in shape [17]. In order to compare the bi-Langmuir and the Langmuir type kinetic models, we fitted the Langmuir kinetic model on the initial part of the experimental curve (dotted line in Fig. 3) and the parameters  $Q_1$  and  $k_{a1}$  were determined by fixing  $k_{d1}$  at  $10^{-3} \text{ s}^{-1}$ . In this case, the simulated front reaches its asymptotic value faster and is located largely above the experimental profile. By contrast, the whole shape of the experimental breakthrough curve is very well fitted by the model that assumes two types of adsorption sites (solid line in Fig. 3). The kinetic

parameters of the Langmuir kinetic model, obtained by fitting the initial portion of the breakthrough curve are close to those determined from the fit of the bi-Langmuir model for the first class of sites.

As the value of the desorption rate constant was roughly estimated from the experimental data, it is interesting to study the effect of fixing different desorption rate values on the other four parameters determined by the least-square fit method (Table 2). At larger apparent desorption rates, one can notice an important increase in the  $Q_2$  values, while the adsorption capacities of the sites of type 1 are not significantly affected. Simultaneously, a larger value of  $k^a_1$  and a lower value of  $k^a_2$  are obtained.

The sum of the square of the differences ( $\Sigma$ ) are also listed in Table 2. These results are compared with those obtained from a model that assumes irreversible adsorption ( $k_{d1}$  and  $k_{d2} < 10^{-4} \text{ s}^{-1}$ ). The fit is excellent for any value of the desorption rates below  $5 \cdot 10^{-3} \text{ s}^{-1}$ . The hypothesis of large desorption rate values ( $7 \cdot 10^{-3} \text{ s}^{-1}$  and above) is unlikely, as the fit is not good. The value of  $1 \cdot 10^{-3} \text{ s}^{-1}$  estimated for the desorption rate from the amount of protein retained in the first and the second adsorption steps is thus quite reasonable and the parameters of Table 1 are close to those obtained with a model that assumes an irreversible adsorption process.

A marked decrease of the affinity for both types of binding sites is noticed for increasing values of the desorption rate constants. When the values of the desorption rate constants are fixed at  $10^{-3} \text{ s}^{-1}$ , the  $K_1$  and  $K_2$  values are typical of a high affinity adsorbent [18]. With larger desorption rate constants, the affinity for the sites of class 1 is still high but that for sites of type 2 is more than 10 times weaker, characteristic of a reversible binding processes.

#### 4.2. Adsorption of a large concentration of $\beta$ -lactoglobulin B

The breakthrough curves for the first and second adsorption analyses of  $\beta$ -lactoglobulin B at  $0.023 \text{ g/l}$  onto the anti- $\beta$ -lactoglobulin column are shown in Fig. 4. The second adsorption analysis was performed after washing the column with the mobile phase buffer for 30 min as indicated in the experimental section. The amount of protein retained in the first adsorption step is  $q=8.0 \mu\text{g}$ , about twice as large as that obtained in the frontal experiment with the diluted protein solution. The shape of the front for the second adsorption analysis is similar to that of the first adsorption analysis: a step front followed by a diffuse part that slowly reaches its asymptotic value. A large amount of protein is still retained, with  $q=6.4 \mu\text{g}$ . The amount of

protein still readsorbed is 80% of the first adsorption step and the desorption rate constant can be estimated to be around  $10^{-3} \text{ s}^{-1}$ .

For both experiments, first and second adsorption steps of  $\beta$ -LG 0.023 g/l, the theoretical profile generated with the bi-Langmuir type kinetic model fits very well the entire breakthrough curves. The theoretical curves of Fig. 4 were obtained by fixing the apparent desorption rate at  $10^{-3} \text{ s}^{-1}$  and determining the other parameters from the best fit of the model to the experimental breakthrough curve. The values of the four kinetic parameters are listed in Table 3. The saturation capacity of the sites of type 1 is lower than one half the value for the sites of type 2. The values of both the apparent adsorption rate and affinity constants for the adsorption on the sites of type 1 are one order of magnitude larger than those on the sites of type 2.

When comparing the kinetic parameters of the first and second adsorption steps, one can notice that the values are not significantly different. Even if the values of  $k_{a2}$  and  $K_2$  are lower in the second adsorption step, they still lie in the same order of magnitude as those of the first adsorption step. This result agrees with the similarity in the shapes of the elution fronts and one can conclude that close adsorption mechanisms take place in the first and second adsorption injections. Most probably, a large amount of protein is desorbed from the column when it is washed by the mobile phase buffer after the first adsorption step, allowing a second adsorption process with kinetic parameters similar to those of the first adsorption step.

The Langmuir kinetic model was fitted to the initial part of the experimental curve for the first adsorption analysis of  $\beta$ -LG 0.023 g/l (dotted line in Fig. 5). As for adsorption at low concentration of  $\beta$ -LG, one can see that the theoretical front reaches its asymptotic value faster and is located largely above the experimental profile. Also, for this large concentration of  $\beta$ -LG, the bi-Langmuir model assuming two types of adsorption sites (solid line in Fig. 5) is more appropriate.

## 5. Discussion

The adsorption of  $\beta$ -LG B onto the polyclonal immunoadsorbent is a complex process. First, the adsorption takes place on a non-uniform adsorbent having a heterogeneous population of binding sites. Second,  $\beta$ -LG B is a self-associating protein [13], [19] and the elution pattern can be affected by the kinetics of interconversion. Finally, a significant amount of the protein is retained by the column in the second adsorption step, as shown in the cyclic adsorption-desorption behavior in Fig. 1. The retention of the protein during the second adsorption analysis

could be explained by partial desorption during the rinsing cycle, allowing an amount of protein to be re-adsorbed. Another interpretation could be the formation of protein multilayers because of protein–protein interaction.

As the Langmuir kinetic model assumes the formation of a monolayer coverage on a homogeneous adsorbent, its application to describe the present adsorption experiments is quite unrealistic. Fig. 3, Fig. 5 show a poor fit between experimental and theoretical results with the Langmuir kinetic model. On the other hand, simulations on the basis of the bi-Langmuir kinetic model represent very well the experimental breakthrough curves.

Although the bi-Langmuir kinetic model is an empirical one for describing the adsorption–desorption kinetic process, the kinetic parameters obtained from the best fit of the model to the experimental front are useful for analyzing the adsorption behavior of  $\beta$ -LG at different experimental conditions. Setting the desorption rate constant at a value of  $10^{-3} \text{ s}^{-1}$  seems reasonable for comparing the adsorption behavior from diluted and concentrated protein solutions. In this work, we considered the possibility of reversible desorption and the fitting procedure was carried out (Table 2, Table 4) by fixing the desorption rate constant at different values. The four kinetic parameters ( $k_{a1}$ ,  $k_{a2}$ ,  $Q_1$ , and  $Q_2$ ) determined from the best fit with desorption rates at  $10^{-3} \text{ s}^{-1}$  (Table 2, Table 4) are close to those obtained with the hypothesis of an irreversible adsorption process, i.e., an extremely slow desorption process with desorption rate values below  $10^{-4} \text{ s}^{-1}$ . Since fits with the bi-Langmuir model are excellent, independently of the value of the desorption rate constant (Table 2, Table 4), it is not possible to select the most appropriate one.

Fixing the desorption rate constants at the value of  $10^{-3} \text{ s}^{-1}$  enables us to compare the kinetic parameters of the bi-Langmuir model obtained at low and large protein concentration. There is a rather good agreement for the parameters of the first term of the adsorption isotherm (high affinity sites), with average  $Q_1=2.4 \text{ mg}$  and  $K_1=108 \text{ l/mol}$ . This is not the case for the parameters of the sites of type 2 (weak affinity sites) as the value of  $Q_2$  is about twice as large for the adsorption of a concentrated  $\beta$ -LG solution. The total column capacity predicted from the experiment performed at  $0.00575 \text{ g/l}$  with the parameters of Table 1 ( $Q_1+Q_2=5 \text{ } \mu\text{g}$ ) is much lower than the actual amount adsorbed ( $q=8.0 \text{ } \mu\text{g}$ ) at a protein concentration of  $0.023 \text{ g/l}$ .

The kinetic model is based upon the assumption of a bi-Langmuir adsorption isotherm (Eq. (4)). At very low concentrations, the adsorption process is mainly depicted by the first term of this equation, i.e., adsorption on the high affinity sites. With the isotherm parameters ( $Q_1=2.4$  mg and  $K_1=108$  l/mol) this first term reaches 95% of its asymptotic value at a protein concentration of 0.002 g/l. For larger concentrations, the variation of the amount adsorbed is mainly due to the second term of the adsorption isotherm equation. In these cases, one can calculate the value of  $K_2$  by considering the variation of the amount adsorbed, from 4.3  $\mu$ g at 0.00575 g/l to 8.0  $\mu$ g at 0.023 g/l. The value estimated for  $K_2$  (around 106 l/mol) is 10 times as low as that predicted by fixing  $k_{d2}$  at  $10^{-3}$  s $^{-1}$  in Table 1, Table 3.

The assumption of equal desorption rates for the low and high affinity sites is certainly too simplistic. Different values were thus assigned to  $k_{d2}$ , and the fitting procedure was carried out for the breakthrough curves performed at low and large protein concentrations. The value selected ( $k_{d2}=5 \cdot 10^{-3}$  s $^{-1}$ ) is the one that gives the lowest deviation between the predicted equilibrium adsorption isotherms at low and large protein concentrations. The four parameters  $Q_1$ ,  $K_1$ ,  $Q_2$ , and  $K_2$  characterizing the adsorption isotherm are listed in Table 5. Fig. 6 shows that the model with  $k_{d1}=1 \cdot 10^{-3}$  s $^{-1}$  and  $k_{d2}=5 \cdot 10^{-3}$  s $^{-1}$  accounts well for both experimental breakthrough curves obtained at low and large protein concentrations in the eluent.

Adsorption on the sites of type 1 is of high affinity, as the value for the adsorption equilibrium constant  $K_1$  is large. The value of  $K_1$  (around 108 l/mol) was calculated with  $k_{d1}=1 \cdot 10^{-3}$  s $^{-1}$ . This is a very rough estimation but a precise  $K_1$  determination requires the direct measurement of the desorption rate constant. The adsorption capacity of the sites of type 1 is relatively low, less than 20% of the total adsorbent capacity. A weak affinity is found for adsorption on the sites of type 2, with a  $K_2$  value around 106 l/mol. The capacity of the sites of type 2 is more than 5 times larger than that of the high affinity sites. At 0.023 g/l, column saturation is not reached as the amount adsorbed ( $q=8$   $\mu$ g) is significantly lower than the total column capacity (10.5  $\mu$ g) calculated with the parameters of Table 5.

The study of adsorption kinetics of  $\beta$ -LG B on a polyclonal immunosorbent carried out by frontal immunochromatography shows that the bi-Langmuir model represents the experimental behavior much better than the simple Langmuir one. The excellent fits obtained do not prove

that this is the only valid theory. The model, being a thermodynamic one, is unable to describe a microscopic picture. This model has to be considered as a simplified description of complex phenomena involving mixed-modes of interactions of the biomolecules with heterogeneous chromatographic supports. Moreover, the assumption of two classes of interacting sites is a simplistic approach for describing the reality of the non-uniform immunoabsorbent.

Because of the fits obtained by considering a reversible or an irreversible adsorption process are of similarly high quality, the type of process that actually takes place cannot be determined. However, experiments including rinsing of the column and reinjection of  $\beta$ -LG B indicate that readsorption of the protein takes place. Further work is necessary to clarify whether partial desorption or multilayer formation of  $\beta$ -LG B is at the origin of this effect.



### **Acknowledgements**

A.P. acknowledges the Spanish Ministry of Science and Technology for a predoctoral grant. This work has been supported by CICYT (project AGL2000-1480). Collaboration between our laboratories has been possible thanks to French–Spanish Cooperation between CNRS and CSIC (project 7954, 2000).

## References

- [1] B. Mariager, M. Solve, H. Eriksen, C.-H. Brogren. *Food Agric. Immunol.*, 6 (1994), p. 73
- [2] Food and Drug Administration Directive, Department of Health and Human Services, Docket No. 95D-0131, Points To Consider in the Manufacture and Testing of Therapeutic Products For Human Use Derived From Transgenic Animals, US Food and Drug Administration, CBER, Rockville, MD (1995)
- [3] M. de Frutos, S.K. Paliwal, F.E. Regnier. *Anal. Chem.*, 65 (1993), p. 2159
- [4] S. Golshan-Shirazi, G. Guiochon. F. Dondi, G. Guiochon (Eds.), *Theoretical Advancement in Chromatography and Related Separation Techniques*, NATO ASI Series, Vol. 383, Kluwer, Dordrecht (1992), p. 35
- [5] A. Jaulmes, C. Vidal-Madjar. *Anal. Chem.*, 63 (1991), p. 1165
- [6] C. Vidal-Madjar, A. Jaulmes. A.J. Milling (Ed.), *Surface Characterization Methods—Principles, Techniques and Applications*, Marcel Dekker, New York (1999), p. 345
- [7] Y. Arata, J. Hirabayashi, K.-I. Kasai. *J. Chromatogr. A*, 905 (2001), p. 337
- [8] A.I. Liapis, B. Anspach, M.E. Findley, J. Davies, M.T.W. Hearn, K.K. Unger. *Biotechnol. Bioeng.*, 34 (1989), p. 467
- [9] B.J. Horstmann, H.A. Chase. *Chem. Eng. Res. Des.*, 67 (1989), p. 243
- [10] H.A. Chase. *J. Chromatogr.*, 297 (1984), p. 179
- [11] Q.M. Mao, A. Johnston, I.G. Prince, M.T.W. Hearn. *J. Chromatogr.*, 548 (1991), p. 147
- [12] A. Jaulmes, C. Vidal-Madjar, A. Pantazaki. *Chromatographia*, 53 (2001), p. S417
- [13] M. de Frutos, A. Cifuentes, J.C. Díez-Masa. *J. Chromatogr. A*, 778 (1997), p. 43
- [14] H.A. McKenzie, W.H. Sawyer. *Nature*, 214 (1967), p. 1101
- [15] P.-O. Larsson, M. Glad, L. Hansson, M.-O. Mansson, S. Ohlson, K. Mosbach. *Adv. Chromatogr.*, 21 (1983), p. 41
- [16] F.H. Arnold, H.W. Blanch, C.R. Wilke. *Chem. Eng. J.*, 30 (1985), p. B25
- [17] J. Renard, C. Vidal-Madjar, C. Lapresle. *J. Colloid Interface Sci.*, 174 (1995), p. 61
- [18] H.E. Swaisgood, I.M. Chaiken. I.M. Chaiken (Ed.), *Analytical Affinity Chromatography*, CRC Press, Boca Raton, FL (1987), p. 65
- [19] R. Lemque, A. Jaulmes, B. Sébille, C. Vidal-Madjar, P. Cysewski. *J. Chromatogr.*, 599 (1992), p. 255

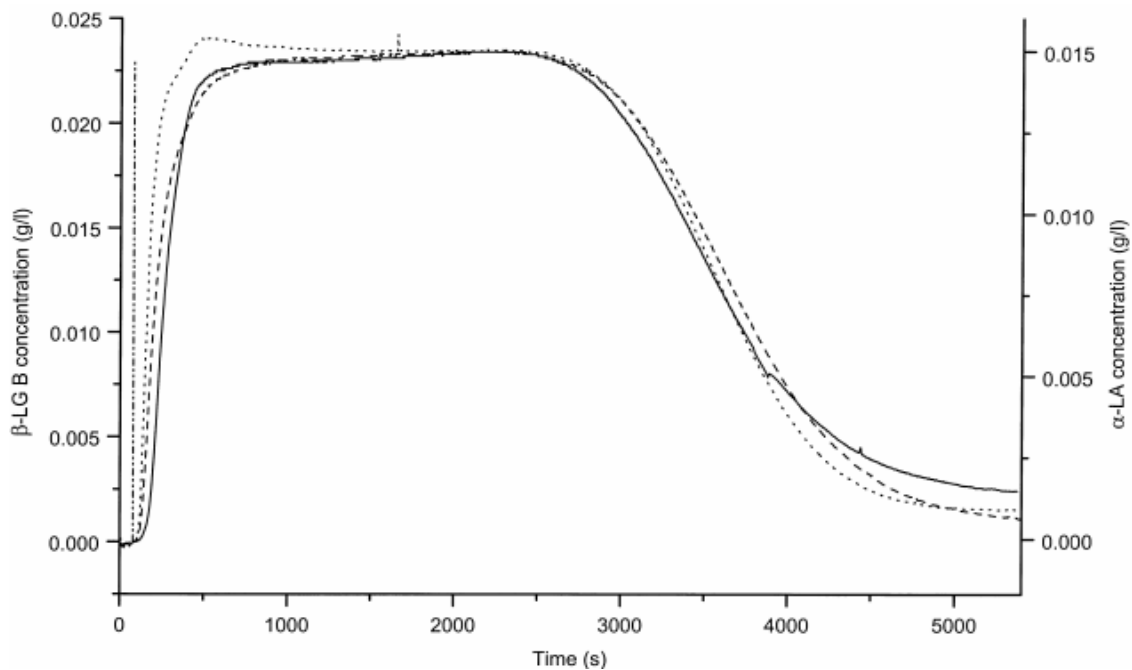


Fig. 1. Frontal adsorption experiments on polyclonal anti- $\beta$ -lactoglobulin covalently bound to aldehyde-silica ( $40\ \mu\text{m}$ ,  $500\ \text{\AA}$ ) packed into a  $5\ \text{cm}\times 2.1\ \text{mm}$  stainless steel HPLC column. (—) first, and (---) second adsorption step (after rinsing the column with the mobile phase buffer for 30 min) of  $\beta$ -LG B ( $C=0.023\ \text{g/l}$ ), and ( $\cdots$ )  $\alpha$ -LA ( $C=0.015\ \text{g/l}$ ). Vertical line (---) corresponds to the  $V_0$  value.

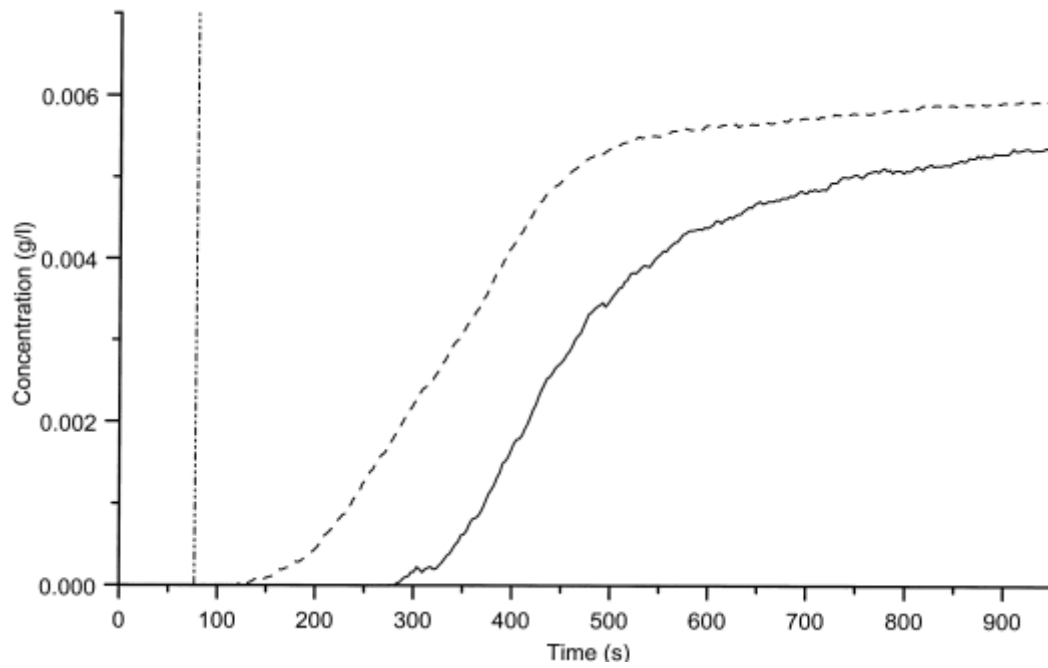


Fig. 2. Comparison of the elution fronts from a diluted  $\beta$ -LG B solution ( $C=0.00575$  g/l). (—) first, and (---) second adsorption step (after rinsing the column with the mobile phase buffer for 30 min). Other experimental conditions as in Fig. 1.

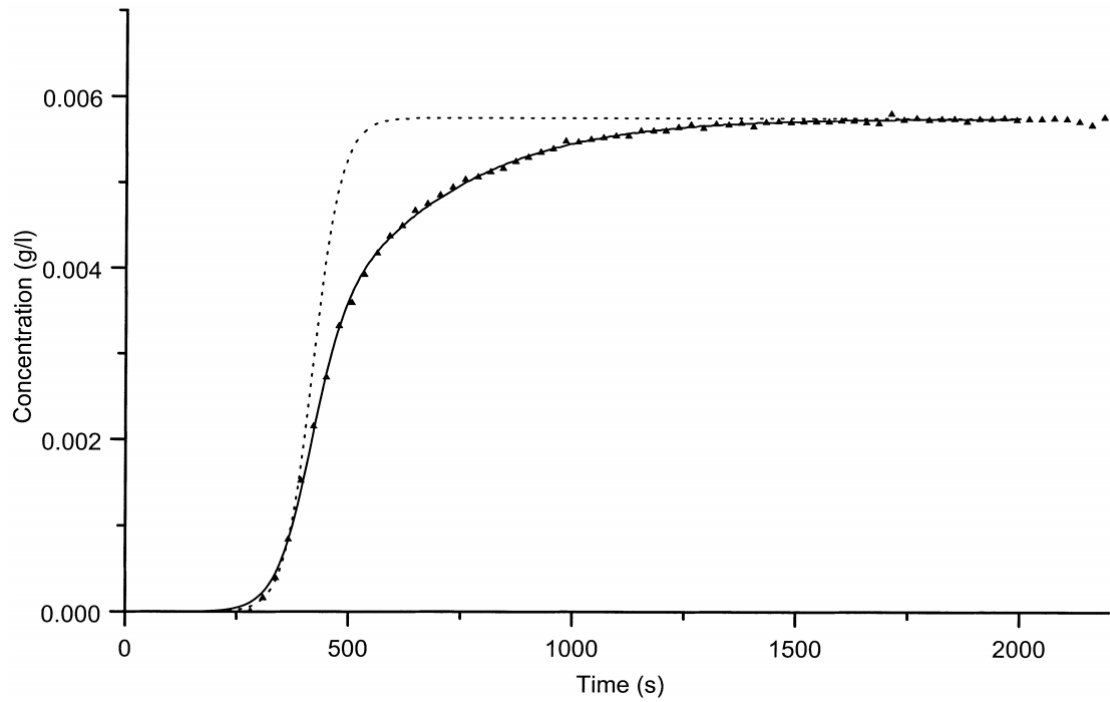


Fig. 3.  $\beta$ -LG B adsorption from a diluted solution ( $C=0.00575$  g/l). ( $\blacktriangle$ ) Experimental; (—) bi-Langmuir, and (----) Langmuir kinetic model. Kinetic parameters of Table 1 with  $k_{d1}=k_{d2}=1 \cdot 10^{-3}$  s $^{-1}$ . Other experimental conditions as in Fig. 1.

Fig. 4.  $\beta$ -LG B adsorption from a concentrated solution ( $C=0.023$  g/l). ( $\blacktriangle$ ) first and ( $\circ$ ) second adsorption step experiment; bi-Langmuir kinetic model (—). Kinetic parameters of Table 3 with  $k_{d1}=k_{d2}=1\cdot 10^{-3}$  s $^{-1}$ . Other experimental conditions as in Fig. 1.

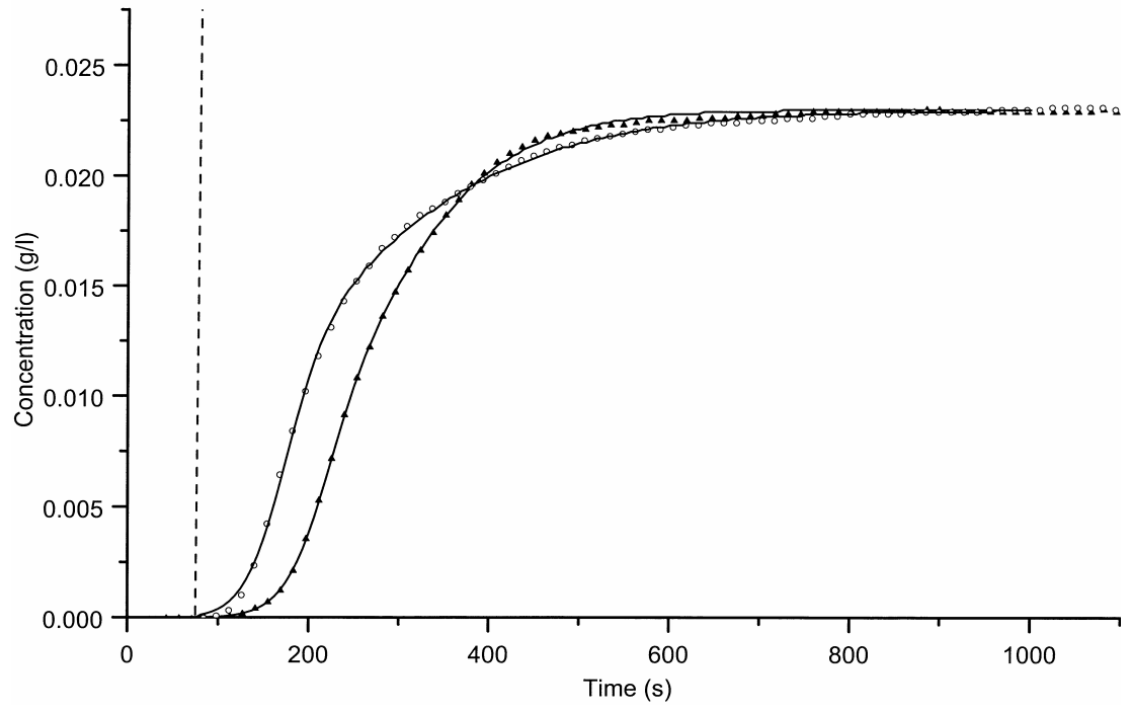
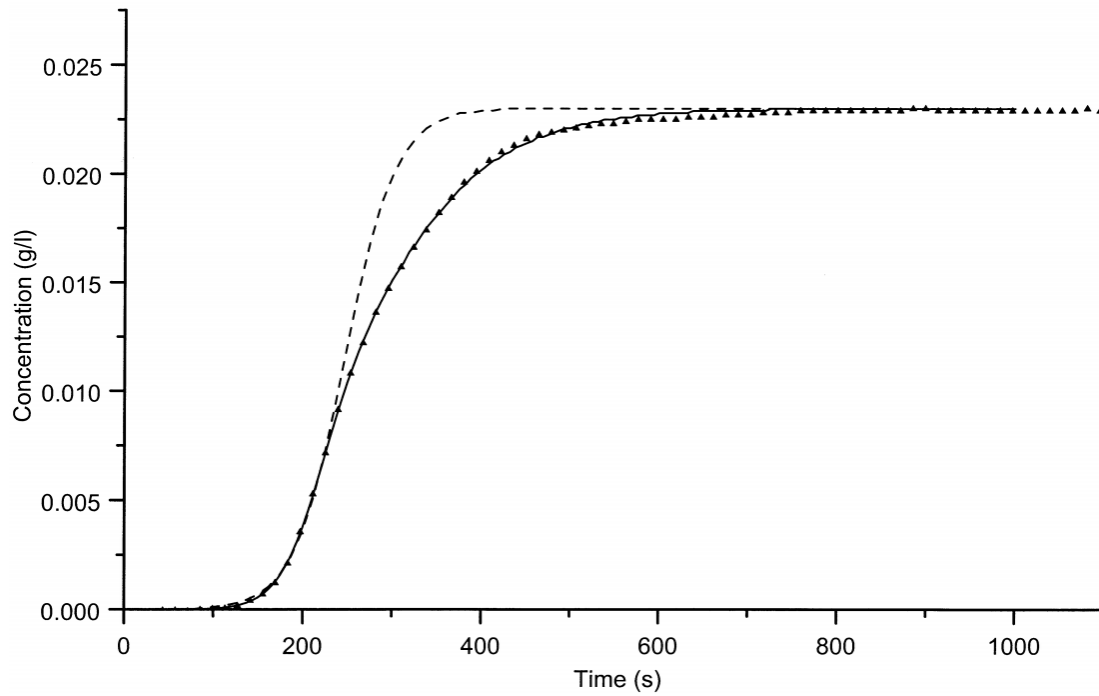


Fig. 5.  $\beta$ -LG B adsorption from a concentrated solution ( $C=0.023$  g/l). ( $\blacktriangle$ ) Experiment, (—) bi-Langmuir, and (----) Langmuir kinetic model. Kinetic parameters of Table 3 with  $k_{d1}=k_{d2}=1 \cdot 10^{-3}$  s $^{-1}$ . Other experimental conditions as in Fig. 1.



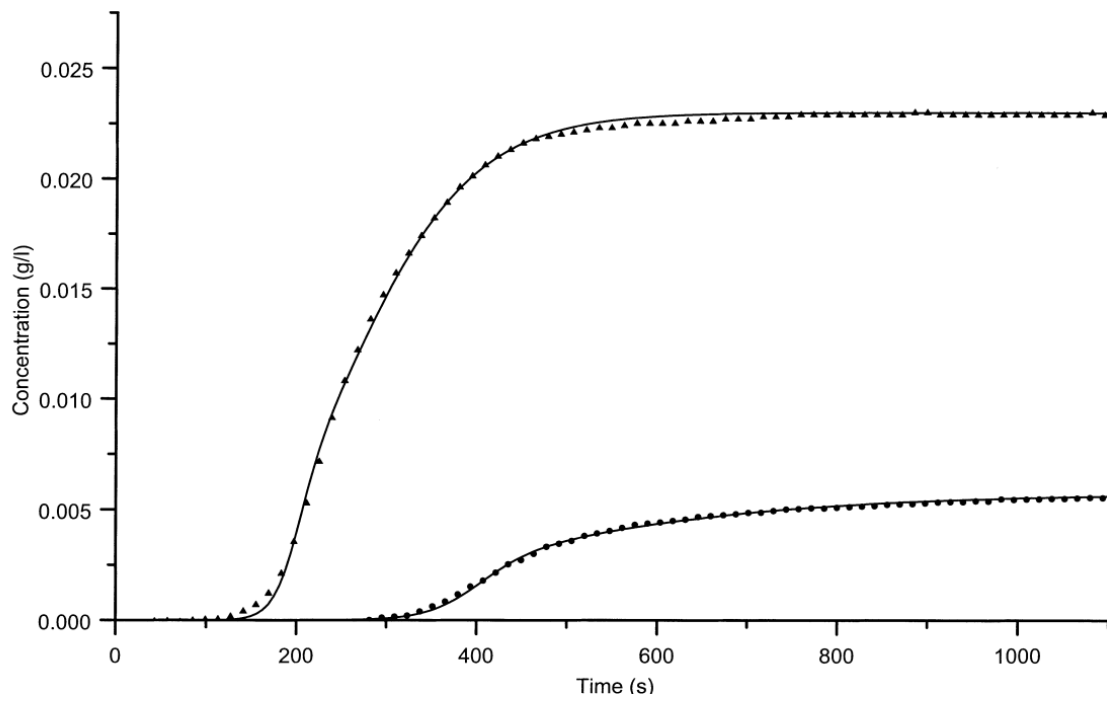


Fig. 6.  $\beta$ -LG B adsorption from a concentrated and a diluted solution. Experiment: (▲)  $C=0.023$  g/l and (●)  $C=0.00575$  g/l, (—) bi-Langmuir kinetic model. Kinetic parameters of Table 5 with  $k_{d1}=10^{-3}$  s $^{-1}$  and  $k_{d2}=5 \cdot 10^{-3}$  s $^{-1}$ . Other experimental conditions as in Fig. 1.



Table 1. Adsorption of a diluted  $\beta$ -LG B solution ( $C=0.00575$  g/l) on the polyclonal anti- $\beta$ -LG column

Adsorption site	Kinetic parameter	Bi-Langmuir model	Langmuir model
Type 1	$Q_1$ ( $\mu\text{g}$ )	2.3	3.4
	$k_1^a$ ( $1 \text{ g}^{-1} \text{ s}^{-1}$ )	6.5	5.4
	$K_1$ ( $1/\text{mol}$ )	$1.2 \cdot 10^8$	$1.0 \cdot 10^8$
Type 2	$Q_2$ ( $\mu\text{g}$ )	2.7	—
	$k_2^a$ ( $1 \text{ g}^{-1} \text{ s}^{-1}$ )	0.6	—
	$K_2$ ( $1/\text{mol}$ )	$1.1 \cdot 10^7$	—

Apparent kinetic parameters with  $k_1^d = k_2^d = 10^{-3} \text{ s}^{-1}$ .

Table 2. Variation of the kinetic parameters obtained from least-square fit with different given values for the apparent desorption rate constant applying the bi-Langmuir model (first adsorption step of  $\beta$ -LG B solution C=0.00575 g/l)

Kinetic parameter	Irreversible adsorption	Reversible adsorption			
$k_1^d$ and $k_2^d$ ( $s^{-1}$ )	$<10^{-4}$	$1 \cdot 10^{-3}$	$2 \cdot 10^{-3}$	$5 \cdot 10^{-3}$	$7 \cdot 10^{-3}$
$Q_1$ ( $\mu g$ )	2.2	2.3	2.4	2.2	1.8
$k_1^a$ ( $l g^{-1} s^{-1}$ )	6.9	6.5	6.9	8.3	11.2
$K_1$ ( $l/mol$ )	$>10^9$	$1.2 \cdot 10^8$	$6.2 \cdot 10^7$	$3.1 \cdot 10^7$	$2.9 \cdot 10^7$
$Q_2$ ( $\mu g$ )	2.1	2.7	3.6	12.1	21.5
$k_2^a$ ( $l g^{-1} s^{-1}$ )	0.77	0.61	0.47	0.20	0.17
$K_2$ ( $l/mol$ )	$>10^8$	$1.1 \cdot 10^7$	$4.2 \cdot 10^6$	$7.2 \cdot 10^5$	$4.4 \cdot 10^5$
$\Sigma$ ( $g/l$ ) <sup>2</sup>	$3.0 \cdot 10^{-6}$	$3.0 \cdot 10^{-6}$	$3.0 \cdot 10^{-6}$	$3.3 \cdot 10^{-6}$	$4.0 \cdot 10^{-6}$

Table 3. Adsorption of a concentrated  $\beta$ -LG B solution ( $C=0.023$  g/l) onto the polyclonal anti- $\beta$ -LG column.

Adsorption site	Kinetic parameter	First adsorption step		Second adsorption step, bi-Langmuir model
		Bi-Langmuir model	Langmuir model	
Type 1	$Q_1$ ( $\mu\text{g}$ )	2.5	6.7	2.2
	$k_1^a$ ( $\text{l g}^{-1} \text{s}^{-1}$ )	3.9	1.5	2.9
	$K_1$ ( $\text{l/mol}$ )	$0.7 \cdot 10^8$	$0.3 \cdot 10^8$	$0.5 \cdot 10^8$
Type 2	$Q_2$ ( $\mu\text{g}$ )	5.6	–	4.8
	$k_2^a$ ( $\text{l g}^{-1} \text{s}^{-1}$ )	0.5	–	0.3
	$K_2$ ( $\text{l/mol}$ )	$1.0 \cdot 10^7$	–	$0.5 \cdot 10^7$

Apparent kinetic parameters with  $k_1^d = k_2^d = 10^{-3} \text{ s}^{-1}$ .

Table 4. Variation of the apparent kinetic parameters obtained from least-square fit with different given values for the desorption rate constant applying the bi-Langmuir model (first adsorption step of  $\beta$ -LG B solution  $C=0.023$  g/l)

Kinetic parameter	Irreversible adsorption	Reversible adsorption			
		$1 \cdot 10^{-3}$	$2 \cdot 10^{-3}$	$5 \cdot 10^{-3}$	$10 \cdot 10^{-3}$
$k_1^d$ and $k_2^d$ ( $s^{-1}$ )	$< 10^{-4}$	$1 \cdot 10^{-3}$	$2 \cdot 10^{-3}$	$5 \cdot 10^{-3}$	$10 \cdot 10^{-3}$
$Q_1$ ( $\mu g$ )	2.8	2.5	2.5	2.5	2.4
$k_1^a$ ( $l g^{-1} s^{-1}$ )	3.1	3.9	3.7	4.0	4.4
$K_1$ ( $l/mol$ )	$> 5 \cdot 10^7$	$7.0 \cdot 10^7$	$3.3 \cdot 10^7$	$1.4 \cdot 10^7$	$7.9 \cdot 10^6$
$Q_2$ ( $\mu g$ )	5.2	5.6	6.4	8.3	7.6
$k_2^a$ ( $l g^{-1} s^{-1}$ )	0.53	0.54	0.51	0.44	0.46
$K_2$ ( $l/mol$ )	$> 10^7$	$9.7 \cdot 10^6$	$4.6 \cdot 10^6$	$1.6 \cdot 10^6$	$8.3 \cdot 10^5$
$\Sigma$ ( $g/l$ ) <sup>2</sup>	$6.4 \cdot 10^{-6}$	$5.0 \cdot 10^{-6}$	$5.0 \cdot 10^{-6}$	$4.8 \cdot 10^{-6}$	$4.8 \cdot 10^{-6}$

Table 5. Adsorption of  $\beta$ -LG B on the polyclonal anti- $\beta$ -LG column

Adsorption site	Kinetic parameter	$\beta$ -LG concentration (g/l)	
		0.00575	0.023
Type 1	$Q_1$ ( $\mu\text{g}$ )	1.8	1.6
	$k_1^a$ ( $\text{l g}^{-1} \text{s}^{-1}$ )	10.1	9.3
	$K_1$ ( $\text{l/mol}$ )	$1.8 \cdot 10^8$	$1.6 \cdot 10^8$
Type 2	$Q_2$ ( $\mu\text{g}$ )	10.3	8.9
	$k_2^a$ ( $\text{l g}^{-1} \text{s}^{-1}$ )	0.28	0.53
	$K_2$ ( $\text{l/mol}$ )	$1.0 \cdot 10^6$	$2.0 \cdot 10^6$
	$\Sigma$ ( $\text{g/l}$ ) <sup>2</sup>	$5.6 \cdot 10^{-5}$	$1.6 \cdot 10^{-5}$

Apparent kinetic parameters with  $k_1^d = 1 \cdot 10^{-3} \text{ s}^{-1}$  and  $k_2^d = 5 \cdot 10^{-3} \text{ s}^{-1}$ .